# CHAPTER VI

# MODEL APPLICATION: A CASE STUDY

In this chapter, the following properties of partially oriented flakeboard mats and oriented strand board (OSB) mats were simulated using ***Winmat***© and analyzed using models developed in the previous chapters: density and overlap profiles, void size distribution, autocorrelation and variance functions, degree of orientations, and thickness swelling. The simulated density and overlap profiles and degree of orientation were compared with those in a commercial OSB panel. In the commercial OSB panel, the density profile was measured by an X-ray scanning technique and the corresponding overlap profile and degree of orientation were estimated from the experimentally determined density profiles. The usefulness and prospective applications of the models were also presented. Future research work and modifications with respect to this model were suggested. Finally, the limitations of the current model are discussed.

## 6.1. Simulation Parameters

The size of the mats simulated here was chosen to be as close as possible to the standard size of commercial panels (2440mm × 1220mm). The flake positions were randomly generated based on the Poisson distribution. The orientation angles of the flakes are also randomly generated as follows: for the partially oriented flakeboard mats, the angles are restricted within $-20^o$ and $+20^o$; for OSB, a three-layer structure is constructed with randomly oriented flakes ($-90^o \leq q \leq +90^o$) in the core and partially oriented flakes (from $-20^o$ to $+20^o$) in both face layers. Details of the simulation parameters are shown in **Table** 6.1. In total 100 mats were simulated for each of the structures by providing different random seeds to the pseudo-random number generator while keeping all the other input parameters unchanged. The results presented hereafter are mean results of all the simulations unless specified otherwise.

**Table** 6.1 Simulation parameters

| Properties | Parameters | |
|---|---|---|
| | Partially oriented flakeboard | OSB |
| Target board size | 2440mm × 1220mm × 11mm | 2440mm × 1220mm × 11mm |
| Target board density | 0.56g/cm$^3$ | 0.56g/cm$^3$ |
| Flake size | 100mm × 15mm × 0.7mm | 100mm × 15mm × 0.7mm |
| Flake density | 0.4g/cm$^3$ | 0.4g/cm$^3$ |
| Flake location | Random | Random |
| Flake orientation | Random (-20$^o$ to +20$^o$) | Faces: random (-20$^o$ to +20$^o$)<br>Core: random (-90$^o$ to +90$^o$) |
| Random number seed | 0 - 99000 (step 1000) | 0 - 99000 (step 1000) |
| Total number of flakes | 43670 | 43670 |
| Total number of layers | 22 | 22 (top 4, core 14, bottom 4) |
| Total flakes in one layer | 1895 | 1895 |
| Replications | 100 | 100 |

Four pieces of 200mm $\times$ 150 mm specimens were cut from a commercial OSB board and the density profile for each specimen was measured by X-ray scanning technique as described in **Chapter** IV. Based on the experimentally measured density profiles, the overlap profiles and the degree of orientation were obtained. The flake geometry as visually viewed from the panel surfaces is roughly rectangular with length in the range of 80 -110 mm and width in the range of 15-30 mm.

## 6.2. Densities and Overlaps

The density and overlap results for the three types of mats were summarized as in **Table** 6.2. From **Table** 6.2, it can be seen that the mean densities for partially oriented flakeboard, simulated OSB, and commercial OSB agreed well. Compared to the commercial OSB, the standard deviation and coefficient of variation of density/overlaps of the simulated mats are higher. **Figure** 6.1 illustrates the comparison of maximum, minimum, mean and standard deviation of density between the simulated and the commercial OSB panels. Although reasonable agreement was noted, there are many unknown assumed variables for the commercial OSB, such as the exact flake geometry, flake density and compression ratio during pressing, which can affect the properties of the final product. **Table** 6.2 also indicates that the overall degrees of orientation for simulated partially oriented flakeboard, simulated OSB and commercial OSB are 66.7%, 40.6% and 42.3%, respectively. Again good agreement was observed in the degrees of orientation of the simulated OSB and the commercial OSB panels.

**Table** 6.2 Basic properties of the mats

| Properties | Simulated partially oriented flakeboard | | Simulated OSB | | Commercial OSB | |
|---|---|---|---|---|---|---|
| | Density ($g/cm^3$) | Overlap | Density ($g/cm^3$) | Overlap | Density ($g/cm^3$) | Overlap |
| Maximum | 1.144 | 44.933 | 1.172 | 46.038 | 1.005 | 39.5 |
| Minimum | 0.124 | 4.885 | 0.119 | 4.678 | 0.156 | 6.129 |
| Mean | 0.560 | 21.989 | 0.560 | 22.006 | 0.556 | 21.852 |
| Standard deviation | 0.117 | 4.581 | 0.116 | 4.558 | 0.077 | 3.032 |
| Coefficient of variation | 20.8% | 20.8% | 20.7% | 20.7% | 13.9% | 13.9% |
| Degree of orientation | 66.7% | | 40.6% | | 42.3% | |

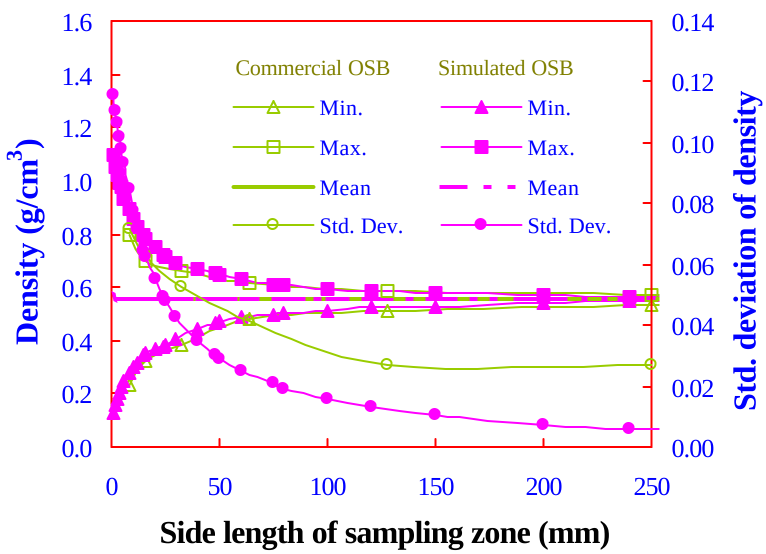


**Figure** 6.1 Density variation of the simulated OSB and the commercial OSB.

### 6.3. Void Area and Distribution

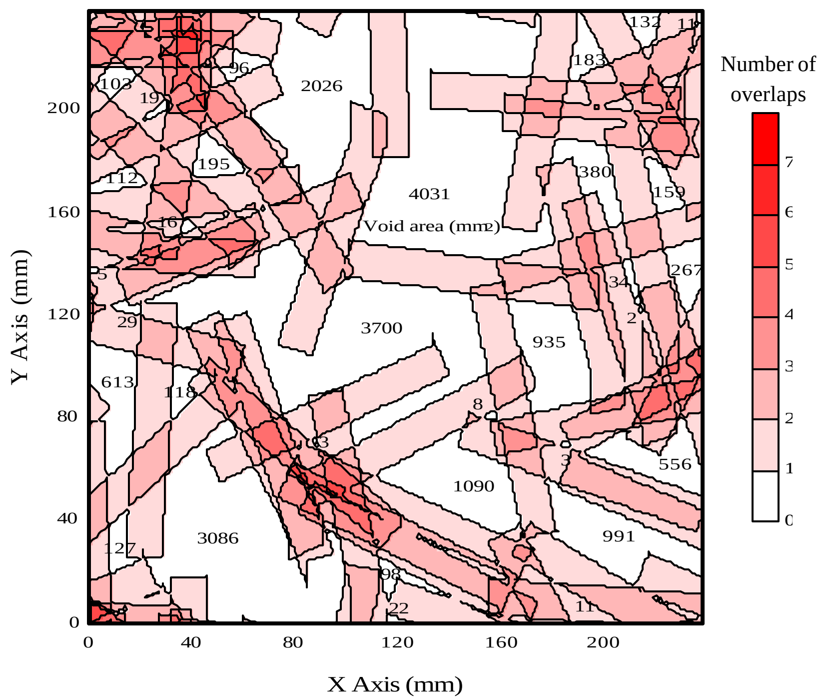


**Figure** 6.2 Void measurement and distribution in a part of a randomly formed layer.

The void areas are determined layer by layer in a loosely formed mat. For example, the voids in 240mm × 240mm sample area cut from one of the randomized layers are counted in **Figure** 6.2 (using ***Winmat***©). The void areas in every layer of simulated partially oriented and simulated OSB mats are listed in **Table** 6.3. It is noted that the voids in the mats are evenly distributed in every layer with very small coefficients of variation (1.1% for partially oriented mat and 1.2% for OSB mat). The total void area in one layer accounts for 37% of the total mat area, which is consistent with the result found in **Chapter** II. In fact, the proportion of voids can be theoretically calculated using the Poisson distribution (Dai and Steiner 1993). By substituting zero overlap ($i$ = 0 means void area) and mean overlap ($l$ = 1 means one layer) into the Poisson distribution $\frac{l^i e^{-l}}{i!} = e^{-1}$, a 36.8% of voids is found in randomly formed flake layer. However, voids in each layer vary in size from 1 $mm^2$ to a maximum of 172,259 $mm^2$ in a partially oriented flake layer and 56,027 $mm^2$ in a random flake layer. In the layers of randomized flake position and orientation, the average void size was smaller than those in the partially oriented layers. This may indicate that the voids are more evenly distributed in the randomized mat than those in the partially oriented mat.

**Table** 6.3 Void areas in the simulated OSB mat and simulated partially oriented mat

| Layer | OSB | | | | Partially oriented board | | | |
|---|---|---|---|---|---|---|---|---|
| | No. of Voids | Total ($mm^2$) | Largest ($mm^2$) | Average ($mm^2$) | No. of Voids | Total ($mm^2$) | Largest ($mm^2$) | Average ($mm^2$) |
| 1 | 832 | 1086970 | 105910 | 1306 | 832 | 1086970 | 105910 | 1306 |
| 2 | 771 | 1122689 | 144486 | 1456 | 771 | 1122689 | 144486 | 1456 |
| 3 | 879 | 1096632 | 57344 | 1248 | 879 | 1096632 | 57344 | 1248 |
| 4 | 800 | 1104965 | 65490 | 1381 | 800 | 1104965 | 65490 | 1381 |
| 5 | 1444 | 1103205 | 34550 | 764 | 826 | 1104529 | 60733 | 1337 |
| 6 | 1483 | 1096443 | 27936 | 739 | 771 | 1094785 | 103771 | 1420 |
| 7 | 1376 | 1125753 | 26494 | 818 | 731 | 1113459 | 140936 | 1523 |
| 8 | 1529 | 1075769 | 38526 | 704 | 855 | 1093203 | 78140 | 1279 |
| 9 | 1495 | 1104380 | 36090 | 739 | 773 | 1111367 | 91969 | 1438 |
| 10 | 1393 | 1113009 | 28638 | 799 | 782 | 1111345 | 111791 | 1421 |
| 11 | 1502 | 1081404 | 42131 | 720 | 846 | 1082779 | 83494 | 1280 |
| 12 | 1474 | 1099458 | 56027 | 746 | 818 | 1088159 | 75255 | 1330 |
| 13 | 1513 | 1081172 | 22820 | 715 | 771 | 1084854 | 133774 | 1407 |
| 14 | 1467 | 1094861 | 28767 | 746 | 876 | 1082058 | 145619 | 1235 |
| 15 | 1477 | 1114037 | 35486 | 754 | 834 | 1108856 | 113862 | 1330 |
| 16 | 1535 | 1083756 | 28044 | 706 | 916 | 1085997 | 72403 | 1186 |

| | | | | | | | | |
|---|---|---|---|---|---|---|---|---|
| 17 | 1450 | 1105746 | 31300 | 763 | 756 | 1109466 | 125464 | 1468 |
| 18 | 1398 | 1099027 | 27208 | 786 | 873 | 1089183 | 64598 | 1248 |
| 19 | 777 | 1113008 | 172259 | 1432 | 777 | 1113008 | 172259 | 1432 |
| 20 | 814 | 1100792 | 83241 | 1352 | 814 | 1100792 | 83241 | 1352 |
| 21 | 745 | 1110078 | 107459 | 1490 | 745 | 1110078 | 107459 | 1490 |
| 22 | 804 | 1097242 | 91678 | 1365 | 804 | 1097242 | 91678 | 1365 |
| Mean | 1467* | 1100473 | 33144* | 750* | 811 | 1099655 | 101348.9 | 1361 |
| Std Dev | 50* | 12930 | 8465* | 34.2* | 48 | 11675 | 31252 | 89 |
| Cov(%) | 3.4* | 1.2 | 25.5* | 4.6* | 5.9 | 1.1 | 30.8 | 6.6 |
| Propor-tion (%) | - | 37.0 | - | - | - | 36.9 | | - |

Note: * These figures evaluated from the 14 core layers of the simulated OSB mat (random orientation). For the face layers, refer to the partially oriented board.

### 6.4. Autocorrelation Functions and Variance Functions

The autocorrelation functions and variance functions can indirectly predict the approximate flake size and flake orientaion in the mats according to the correlation patterns (**Figures** 6.3 and 6.4). This is extremely useful when the information contained in the commercial panels is needed to predict other properties of the mats. For example, the size and orientation of flakes in OSB products are important indicators of key panel strength properties. Mats with shorter flakes have lower strength than mats with longer flakes. The axial strength in a highly oriented board is higher than that in a randomly formed board. **Figures** 6.5 and 6.6 show the autocorrelation functions and variance functions of the simulated partially oriented flakeboard, simulated OSB and commercial OSB in relation to the side length of sampling zones. From **Figures** 6.5 and 6.6, the first part (side length of sampling zone is less than 15 mm) of the autocorrelation function from the commercial OSB is below the random case. This is because all the mathematical predictions and simulations were made based on the assumed uniform flake size of length 100 mm and width 15 mm. There are a lot of fines contained in the commercial OSB panel which are ignored in our models. The autocorrelation curve for commercial OSB also suggests that the flake width may not be the same as that which was used in the simulation process. The prediction and simulation results agree well in both cases.

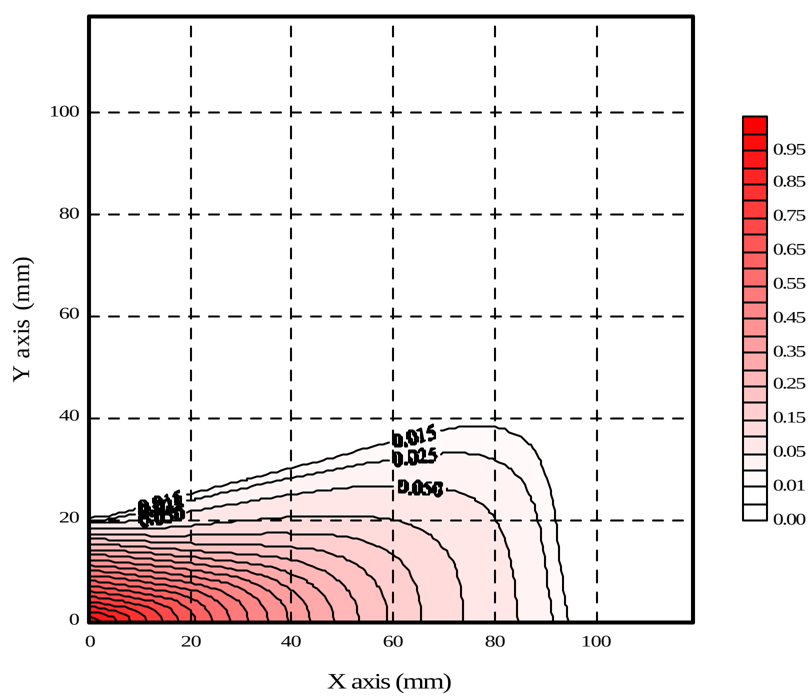


**Figure** 6.3 Autocorrelation function for the simulated partially oriented flakeboard

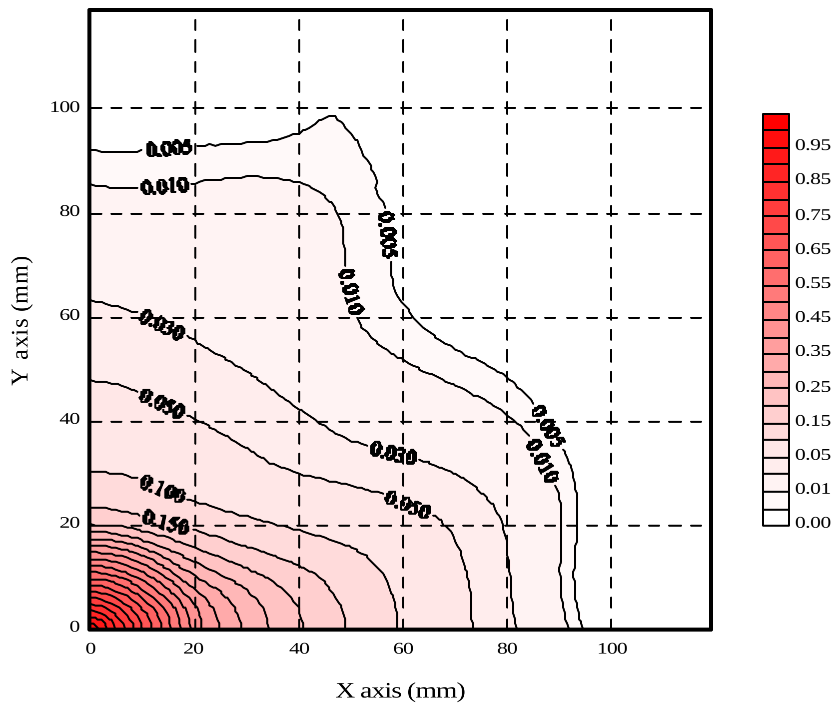


**Figure** 6.4 Autocorrelation function for the simulated OSB

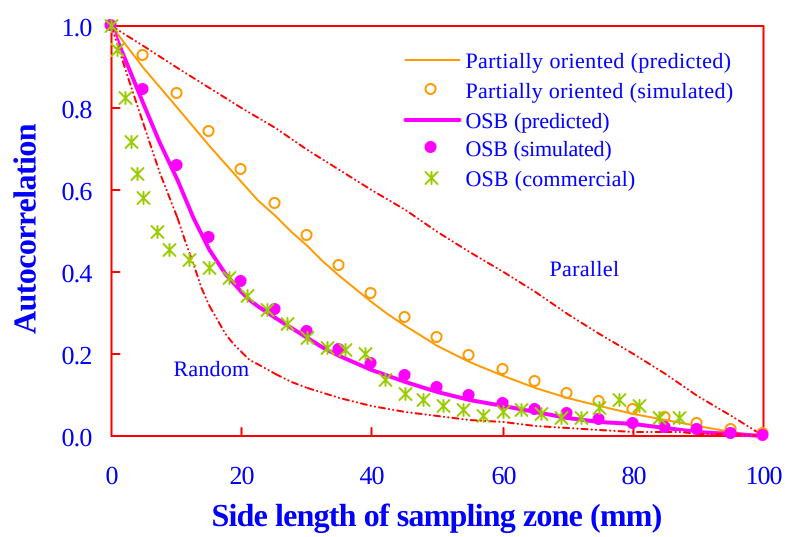


**Figure** 6.5 Autocorrelation functions of the simulated partially oriented flakeboard, the simulated OSB and the commercial OSB.

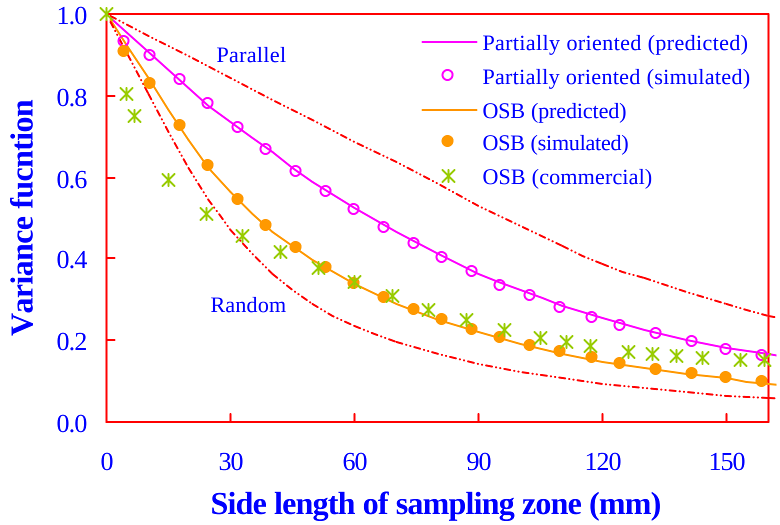


**Figure** 6.6 Variance functions of the silmulated partially oriented flakeboard, the simulated OSB, and the commercial OSB.

## 6.5. Prediction of Thickness Swelling

By applying the results from **Chapter** V, the thickness swelling of the simulated partially oriented flakeboard, and simulated full-size OSB without wax can be predicted, assuming that the compressed mats have 5% initial moisture content and 12% additional moisture absorption under 95% relative humidity condition and 10% additional moisture absorption under 90% relative humidity condition (**Table** 6.4). The 12% and 10% moisture absorption is chosen because it is close to the equilibrium moisture absorption in the corresponding conditions. Based on the predicted results, it can be noted that the thickness swelling within a mat is also randomly distributed in the horizontal direction (**Figures** 6.7a, 6.7b, 6.8a and 6.8b). The predicted average value of thickness swelling under 95% RH condition is 25.75%

for the simulated partially oriented flakeboard and 24.79% for the simulated OSB, respectively (**Table** 6.4). The thickness swelling is about 23% less when the samples are considered under 90% RH than under 95% RH condition. **Table** 6.5 lists the average values of thickness swelling of simulated OSB in each sampling zone of 50mm × 50mm under the condition of 95% relative humidity exposure.

**Table** 6.4 Predicted thickness swelling under 95% and 90% relative humidity conditions

| Properties (%) | Simulated partially oriented flakeboard | | Simulated OSB | | Commercial OSB | |
|---|---|---|---|---|---|---|
| | 95% RH | 90% RH | 95% RH | 90% RH | 95% RH | 90% RH |
| Maximum | 31.5 | 24.7 | 30.9 | 24.2 | 24.7 | 19.0 |
| Minimum | 19.3 | 14.5 | 18.3 | 13.7 | 20.2 | 15.2 |
| Mean | 25.8 | 19.9 | 24.8 | 19.1 | 22.7 | 17.3 |
| Standard deviation | 2.0 | 1.7 | 1.9 | 1.6 | 1.0 | 0.9 |
| Coefficient of variation | 7.8 | 8.4 | 7.7 | 8.4 | 4.6 | 5.1 |

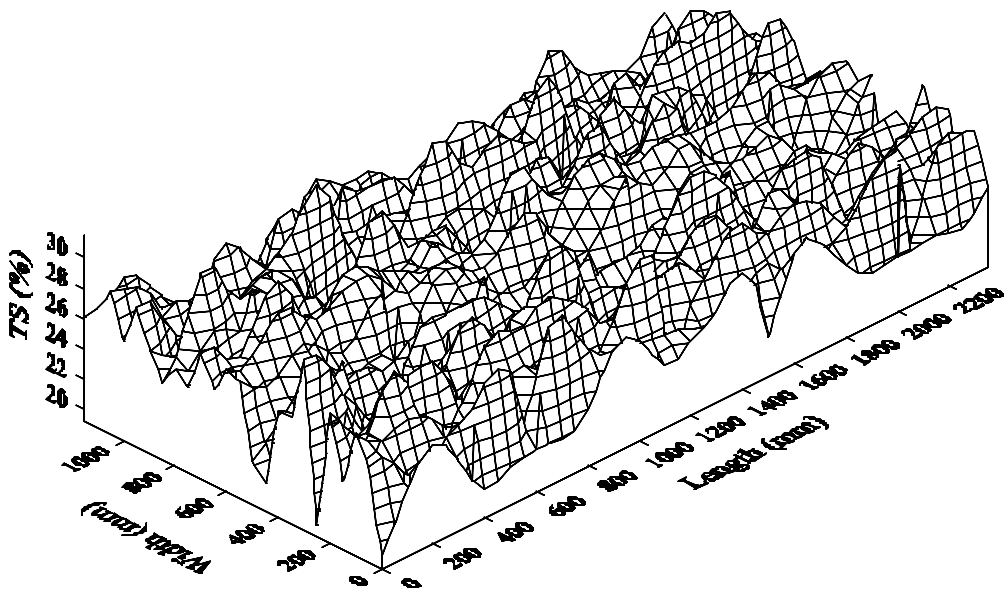


**Figure** 6.7a 3D representation of the predicted thickness swelling of the simulated partially oriented flakeboard under 95% relative humidity condition.

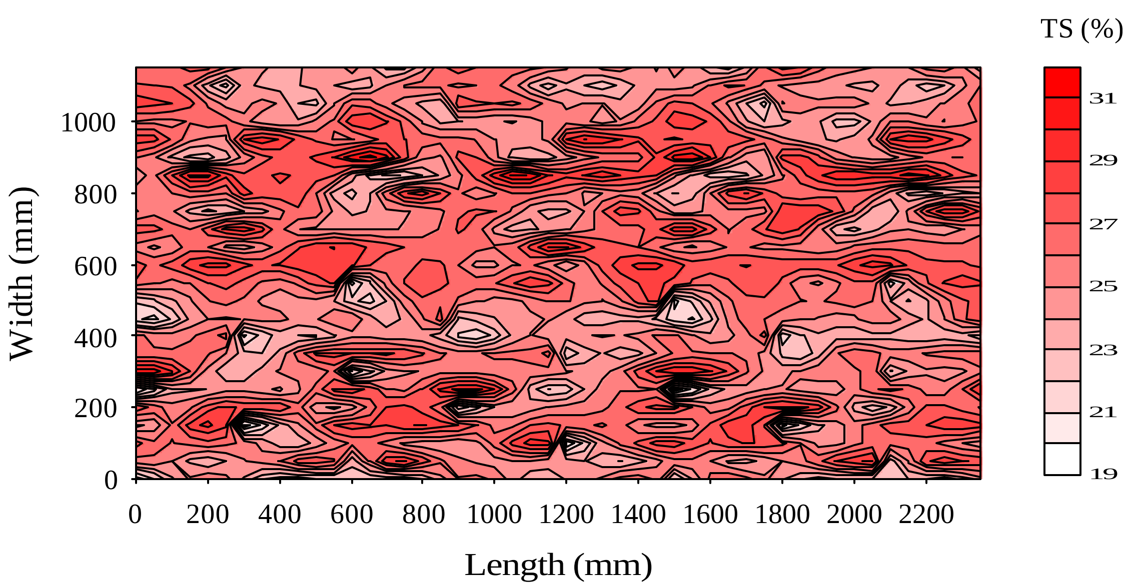


**Figure** 6.7b 2D representation of the predicted thickness swelling of the simulated partially oriented flakeboard under 95% relative humidity condition.

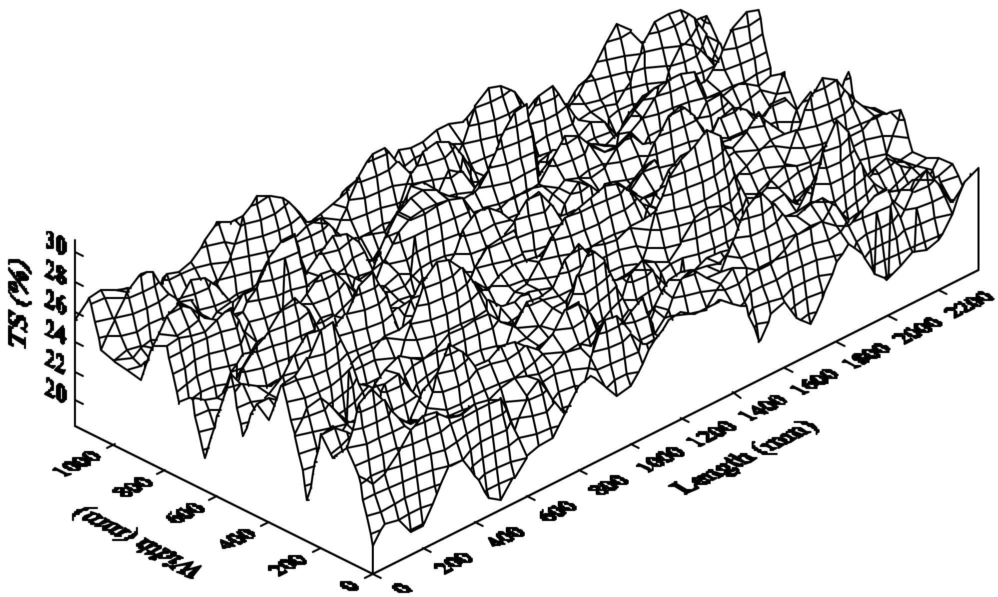


**Figure** 6.8a  3D representation of the predicted thickness swelling of the simulated OSB under 90% relative humidity condition.

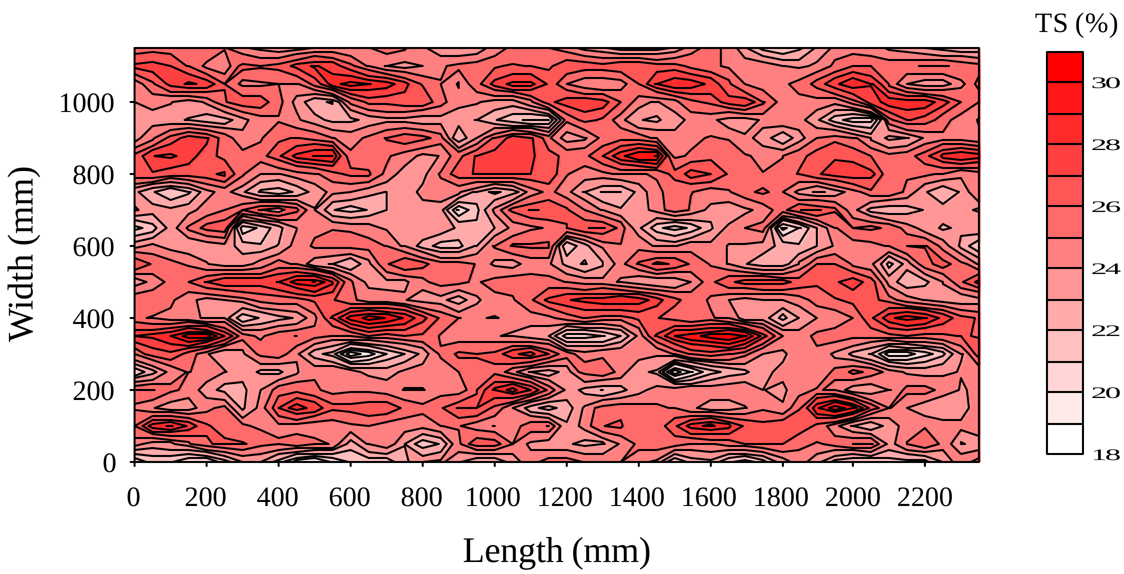


**Figure** 6.8b  2D representation of the predicted thickness swelling of the simulated OSB under 90% relative humidity condition.

**Table** 6.5 Distribution of thickness swelling of simulated OSB in horizontal plane (sampling zone: 50mm × 50mm)*

| ** | 1 | 2 | 3 | 4 | 5 | 6 | 7 | 8 | 9 | 10 | 11 | 12 | 13 | 14 | 15 | 16 | 17 | 18 | 19 | 20 | 21 | 22 | 23 | 24 |
|---|---|---|---|---|---|---|---|---|---|---|---|---|---|---|---|---|---|---|---|---|---|---|---|---|
| **1** | 20.2 | 20.9 | 22.4 | 23.7 | 23.2 | 22.7 | 24.1 | 24.2 | 21.1 | 18.4 | 18.3 | 19.3 | 20.4 | 21.2 | 21.5 | 22.3 | 23.3 | 23.1 | 22.0 | 21.6 | 21.1 | 20.2 | 19.7 | 19.9 |
| **2** | 21.3 | 22.4 | 24.2 | 25.1 | 24.3 | 24.2 | 25.9 | 25.8 | 22.5 | 19.9 | 19.5 | 19.7 | 20.5 | 22.0 | 23.1 | 23.8 | 24.4 | 24.1 | 23.7 | 23.5 | 22.6 | 21.2 | 21.0 | 21.6 |
| **3** | 21.2 | 22.8 | 24.9 | 25.9 | 26.0 | 27.0 | 28.9 | 28.1 | 24.3 | 21.6 | 20.9 | 20.5 | 20.9 | 22.6 | 24.1 | 24.7 | 25.3 | 25.6 | 25.9 | 25.7 | 24.2 | 22.6 | 23.0 | 24.3 |
| **4** | 19.9 | 21.2 | 23.1 | 24.6 | 26.2 | 28.6 | 30.7 | 29.4 | 25.0 | 22.3 | 22.0 | 21.8 | 21.9 | 23.1 | 24.1 | 24.8 | 26.0 | 26.8 | 27.0 | 26.5 | 24.9 | 23.9 | 25.0 | 26.4 |
| **5** | 19.9 | 20.4 | 21.3 | 22.9 | 25.2 | 27.7 | 29.4 | 28.2 | 24.7 | 22.8 | 23.3 | 24.0 | 24.2 | 24.6 | 25.0 | 25.9 | 27.1 | 27.4 | 26.4 | 25.4 | 24.7 | 24.8 | 26.0 | 27.1 |
| **6** | 21.5 | 21.7 | 22.0 | 23.4 | 25.1 | 26.3 | 26.7 | 25.8 | 24.1 | 23.7 | 25.1 | 26.6 | 27.1 | 27.1 | 26.9 | 27.2 | 28.0 | 27.5 | 25.4 | 23.8 | 23.8 | 24.9 | 26.2 | 26.9 |
| **7** | 23.0 | 23.6 | 24.7 | 25.9 | 26.7 | 26.3 | 25.0 | 24.0 | 23.6 | 24.3 | 26.2 | 28.1 | 29.0 | 29.3 | 28.8 | 27.9 | 27.9 | 27.3 | 25.3 | 23.7 | 23.9 | 24.9 | 25.7 | 26.2 |
| **8** | 23.0 | 24.4 | 26.8 | 28.5 | 28.6 | 26.7 | 24.0 | 22.5 | 22.9 | 24.1 | 26.1 | 28.2 | 29.7 | 30.3 | 29.6 | 28.2 | 27.5 | 26.7 | 25.0 | 24.2 | 24.5 | 24.5 | 24.6 | 25.0 |
| **9** | 21.5 | 23.4 | 26.6 | 29.2 | 29.2 | 26.6 | 23.3 | 22.0 | 22.7 | 24.1 | 26.3 | 28.9 | 30.3 | 30.0 | 29.1 | 28.5 | 28.0 | 26.1 | 23.8 | 23.7 | 24.5 | 23.8 | 23.4 | 23.9 |
| **10** | 19.6 | 21.6 | 25.0 | 27.9 | 28.2 | 25.8 | 23.1 | 22.7 | 23.8 | 25.3 | 27.8 | 30.5 | 30.9 | 28.9 | 27.7 | 28.8 | 29.5 | 26.8 | 23.5 | 23.2 | 24.0 | 23.4 | 22.9 | 23.1 |
| **11** | 19.0 | 20.8 | 23.8 | 26.2 | 26.8 | 25.2 | 23.5 | 23.6 | 24.9 | 26.3 | 28.4 | 30.5 | 30.1 | 27.4 | 26.4 | 28.6 | 30.0 | 27.7 | 24.4 | 23.5 | 23.9 | 23.7 | 23.3 | 23.3 |
| **12** | 20.0 | 21.3 | 23.4 | 25.4 | 26.4 | 25.8 | 24.7 | 24.4 | 24.9 | 25.7 | 27.1 | 28.1 | 27.5 | 25.9 | 25.8 | 27.5 | 28.2 | 26.4 | 24.3 | 23.5 | 23.6 | 23.7 | 24.0 | 24.5 |
| **13** | 21.1 | 21.7 | 23.2 | 25.2 | 26.8 | 27.0 | 26.0 | 24.9 | 24.4 | 24.6 | 25.3 | 25.5 | 25.0 | 25.0 | 25.9 | 26.3 | 25.2 | 23.6 | 22.7 | 22.5 | 22.6 | 22.9 | 24.2 | 25.6 |
| **14** | 21.2 | 21.5 | 22.7 | 24.8 | 26.7 | 27.0 | 26.1 | 24.8 | 23.8 | 23.8 | 24.6 | 24.8 | 24.5 | 24.9 | 25.9 | 25.6 | 23.7 | 22.1 | 21.9 | 22.1 | 22.1 | 22.3 | 23.5 | 24.9 |
| **15** | 21.4 | 21.7 | 22.9 | 24.6 | 25.8 | 25.8 | 25.4 | 24.6 | 23.6 | 23.6 | 24.8 | 25.6 | 25.3 | 25.0 | 25.2 | 24.9 | 23.6 | 22.8 | 22.9 | 23.0 | 23.0 | 23.0 | 23.2 | 23.6 |
| **16** | 22.6 | 23.0 | 24.0 | 24.6 | 24.3 | 24.1 | 24.6 | 24.8 | 24.2 | 23.9 | 25.0 | 26.0 | 25.8 | 24.8 | 24.2 | 24.0 | 23.8 | 24.1 | 24.5 | 24.4 | 24.2 | 24.2 | 23.7 | 23.3 |
| **17** | 24.0 | 24.7 | 25.3 | 24.4 | 22.8 | 22.4 | 23.6 | 24.7 | 24.6 | 24.0 | 24.5 | 25.4 | 25.4 | 24.5 | 23.8 | 23.8 | 24.6 | 25.8 | 26.2 | 25.2 | 24.6 | 24.7 | 24.3 | 23.7 |
| **18** | 24.3 | 25.3 | 25.8 | 24.4 | 22.3 | 21.6 | 22.5 | 24.0 | 24.6 | 24.2 | 24.2 | 24.9 | 25.2 | 24.7 | 24.0 | 24.0 | 25.5 | 27.4 | 27.2 | 25.4 | 24.6 | 25.1 | 25.0 | 24.4 |
| **19** | 23.1 | 24.5 | 25.5 | 24.8 | 23.3 | 22.4 | 22.6 | 23.8 | 25.0 | 25.2 | 25.0 | 25.4 | 25.7 | 25.5 | 24.6 | 24.0 | 25.2 | 27.1 | 26.9 | 25.4 | 25.1 | 25.9 | 26.0 | 25.7 |
| **20** | 22.1 | 23.6 | 24.9 | 25.0 | 24.6 | 24.2 | 24.0 | 24.5 | 25.8 | 26.5 | 26.2 | 25.8 | 26.0 | 26.0 | 25.3 | 24.5 | 24.8 | 25.9 | 25.9 | 25.4 | 26.0 | 26.9 | 27.1 | 27.0 |
| **21** | 22.2 | 23.8 | 24.8 | 24.7 | 24.9 | 25.5 | 25.5 | 25.1 | 25.7 | 26.7 | 26.5 | 25.8 | 25.6 | 25.7 | 25.6 | 25.4 | 25.5 | 25.3 | 24.9 | 25.0 | 26.0 | 27.1 | 27.4 | 27.2 |
| **22** | 23.4 | 24.8 | 25.4 | 24.4 | 24.4 | 25.6 | 25.8 | 24.6 | 24.5 | 25.7 | 26.2 | 25.9 | 25.7 | 25.6 | 25.7 | 25.9 | 25.8 | 24.9 | 24.0 | 23.8 | 24.6 | 25.8 | 26.3 | 26.2 |
| **23** | 24.6 | 25.8 | 26.0 | 24.6 | 24.3 | 25.3 | 25.1 | 23.5 | 23.0 | 24.2 | 25.3 | 25.8 | 26.1 | 26.1 | 26.1 | 26.2 | 25.5 | 24.1 | 23.0 | 22.6 | 22.7 | 23.4 | 24.1 | 24.3 |
| **24** | 25.4 | 26.3 | 26.2 | 25.0 | 24.7 | 25.2 | 24.7 | 23.1 | 22.3 | 23.1 | 23.9 | 24.9 | 25.9 | 26.1 | 26.1 | 26.3 | 25.4 | 23.4 | 22.2 | 21.7 | 21.1 | 21.3 | 22.1 | 22.6 |
| **25** | 25.5 | 26.2 | 26.0 | 25.1 | 24.8 | 24.9 | 24.7 | 24.0 | 23.5 | 23.6 | 23.7 | 24.3 | 25.3 | 25.5 | 25.3 | 25.5 | 25.0 | 23.4 | 22.3 | 21.5 | 20.5 | 20.5 | 21.5 | 22.1 |
| **26** | 24.9 | 25.4 | 25.3 | 24.6 | 24.1 | 24.2 | 24.8 | 25.3 | 25.5 | 25.4 | 24.7 | 24.3 | 24.9 | 25.1 | 24.5 | 24.4 | 24.5 | 24.4 | 24.1 | 23.0 | 21.5 | 21.2 | 22.0 | 22.5 |
| **27** | 24.9 | 25.1 | 24.9 | 24.0 | 23.3 | 23.5 | 24.5 | 25.5 | 26.0 | 25.8 | 24.8 | 24.2 | 24.7 | 25.1 | 24.4 | 23.9 | 24.4 | 25.4 | 26.0 | 25.1 | 23.4 | 22.7 | 23.0 | 23.1 |
| **28** | 25.0 | 25.5 | 25.4 | 24.4 | 23.4 | 23.4 | 24.0 | 24.5 | 24.6 | 24.2 | 23.7 | 23.8 | 24.4 | 24.7 | 24.1 | 23.7 | 23.9 | 24.9 | 26.0 | 26.1 | 25.2 | 24.2 | 23.6 | 23.5 |
| **29** | 24.4 | 25.3 | 26.0 | 25.5 | 24.5 | 24.0 | 23.9 | 23.9 | 23.2 | 22.5 | 22.7 | 23.4 | 23.8 | 23.6 | 23.3 | 23.2 | 23.1 | 23.4 | 24.7 | 26.2 | 26.4 | 25.0 | 23.7 | 23.3 |
| **30** | 23.7 | 24.9 | 26.0 | 26.1 | 25.4 | 24.8 | 24.6 | 24.2 | 22.9 | 21.6 | 21.9 | 23.1 | 23.8 | 23.7 | 23.5 | 23.5 | 23.1 | 22.9 | 24.2 | 26.3 | 26.8 | 25.3 | 23.6 | 22.8 |
| **31** | 23.3 | 24.3 | 25.1 | 25.2 | 25.1 | 25.1 | 25.1 | 24.8 | 23.5 | 22.1 | 22.2 | 23.6 | 25.2 | 25.7 | 25.2 | 24.7 | 24.3 | 23.9 | 24.7 | 26.4 | 26.9 | 25.5 | 23.9 | 23.2 |
| **32** | 22.1 | 22.8 | 23.6 | 24.0 | 24.5 | 25.1 | 25.2 | 25.1 | 24.7 | 23.9 | 23.6 | 24.6 | 26.4 | 27.1 | 26.3 | 25.7 | 25.9 | 25.6 | 25.4 | 26.1 | 26.6 | 25.8 | 24.9 | 24.5 |
| **33** | 21.1 | 21.7 | 22.8 | 23.9 | 24.8 | 25.1 | 25.2 | 25.7 | 26.3 | 26.0 | 25.1 | 24.9 | 25.9 | 26.6 | 26.2 | 26.3 | 27.3 | 27.3 | 26.4 | 26.3 | 26.6 | 26.1 | 25.6 | 25.5 |
| **34** | 21.8 | 22.4 | 23.3 | 24.4 | 25.1 | 24.9 | 24.6 | 25.8 | 27.5 | 27.5 | 25.7 | 24.2 | 24.3 | 25.4 | 26.5 | 27.5 | 28.2 | 28.3 | 27.9 | 27.4 | 26.9 | 26.1 | 25.2 | 24.8 |
| **35** | 23.6 | 24.3 | 24.6 | 24.8 | 24.9 | 24.2 | 23.7 | 25.1 | 27.3 | 27.3 | 25.3 | 23.4 | 23.1 | 24.5 | 26.7 | 27.8 | 27.8 | 28.3 | 28.8 | 28.1 | 26.9 | 25.7 | 24.3 | 23.1 |
| **36** | 24.4 | 25.3 | 25.8 | 25.5 | 25.1 | 24.5 | 24.0 | 24.6 | 25.6 | 25.3 | 23.9 | 22.8 | 22.8 | 23.9 | 25.5 | 26.1 | 26.1 | 27.0 | 28.1 | 27.7 | 26.6 | 25.5 | 23.4 | 21.5 |
| **37** | 23.2 | 24.5 | 25.9 | 26.4 | 26.4 | 26.3 | 25.7 | 24.9 | 24.3 | 23.5 | 22.6 | 22.7 | 23.5 | 24.0 | 24.3 | 24.6 | 24.7 | 25.0 | 25.8 | 26.3 | 26.3 | 25.5 | 23.1 | 20.9 |
| **38** | 21.9 | 23.0 | 24.7 | 26.2 | 27.4 | 28.0 | 27.1 | 25.7 | 24.8 | 23.8 | 22.9 | 23.3 | 24.4 | 24.3 | 24.1 | 24.7 | 24.8 | 24.1 | 24.0 | 24.9 | 25.8 | 25.5 | 23.5 | 21.7 |
| **39** | 21.5 | 22.0 | 23.0 | 24.8 | 27.0 | 28.2 | 27.6 | 26.4 | 25.8 | 25.3 | 24.1 | 23.8 | 24.3 | 24.1 | 23.8 | 24.6 | 25.0 | 24.0 | 23.3 | 23.9 | 25.2 | 25.6 | 24.3 | 23.2 |
| **40** | 22.1 | 22.0 | 22.2 | 23.6 | 25.9 | 27.5 | 27.6 | 26.8 | 26.1 | 25.8 | 24.8 | 23.6 | 23.4 | 23.5 | 23.5 | 24.3 | 24.9 | 24.4 | 23.5 | 23.6 | 24.9 | 25.9 | 25.2 | 24.3 |
| **41** | 23.4 | 23.2 | 23.1 | 23.7 | 25.0 | 26.5 | 27.2 | 26.6 | 25.7 | 25.4 | 24.6 | 23.3 | 23.3 | 24.1 | 24.6 | 25.4 | 26.2 | 26.0 | 24.8 | 24.0 | 24.8 | 25.9 | 25.5 | 24.6 |

| ** | 1 | 2 | 3 | 4 | 5 | 6 | 7 | 8 | 9 | 10 | 11 | 12 | 13 | 14 | 15 | 16 | 17 | 18 | 19 | 20 | 21 | 22 | 23 | 24 |
|---|---|---|---|---|---|---|---|---|---|---|---|---|---|---|---|---|---|---|---|---|---|---|---|---|
| **42** | 24.3 | 24.7 | 25.2 | 25.1 | 25.0 | 25.7 | 26.4 | 26.0 | 25.1 | 24.8 | 24.2 | 23.4 | 24.3 | 25.9 | 26.6 | 27.5 | 28.5 | 28.1 | 26.4 | 24.8 | 24.5 | 25.1 | 25.0 | 24.3 |
| **43** | 24.0 | 25.3 | 26.7 | 26.6 | 25.6 | 25.4 | 25.7 | 25.3 | 24.7 | 24.4 | 23.8 | 23.5 | 24.9 | 26.8 | 27.6 | 28.5 | 29.4 | 29.0 | 27.3 | 25.3 | 24.0 | 24.2 | 24.3 | 23.9 |
| **44** | 23.3 | 25.0 | 26.9 | 27.1 | 26.1 | 25.6 | 25.7 | 25.5 | 25.2 | 24.8 | 23.7 | 23.0 | 24.4 | 26.6 | 27.9 | 28.7 | 29.1 | 28.7 | 27.5 | 25.5 | 23.8 | 23.6 | 23.8 | 23.4 |
| **45** | 23.0 | 24.6 | 26.5 | 27.2 | 26.9 | 26.7 | 26.8 | 26.7 | 26.1 | 25.1 | 23.4 | 22.2 | 23.1 | 25.5 | 27.5 | 28.5 | 28.5 | 27.8 | 27.1 | 25.9 | 24.2 | 23.3 | 23.2 | 23.0 |
| **46** | 23.4 | 24.8 | 26.4 | 27.2 | 27.7 | 28.3 | 28.7 | 28.2 | 26.8 | 24.9 | 22.9 | 21.3 | 21.4 | 23.7 | 26.1 | 27.5 | 27.4 | 26.3 | 25.9 | 26.1 | 25.3 | 23.6 | 22.7 | 22.6 |
| **47** | 24.2 | 25.7 | 26.8 | 27.0 | 27.7 | 29.1 | 29.9 | 28.9 | 26.4 | 24.2 | 22.6 | 20.8 | 20.5 | 22.2 | 24.5 | 25.9 | 25.9 | 24.9 | 24.7 | 25.9 | 26.0 | 24.0 | 22.5 | 22.4 |
| **48** | 24.6 | 26.3 | 27.2 | 26.8 | 27.4 | 29.1 | 30.0 | 28.4 | 25.6 | 23.6 | 22.5 | 21.0 | 20.5 | 21.9 | 23.8 | 24.9 | 25.1 | 24.3 | 24.3 | 25.7 | 26.0 | 24.1 | 22.5 | 22.3 |

* The thickness swelling is predicted under the condition of 95% relative humidity exposure.

** The numbers in the first row and the first column in this table represent the location of each sampling zone by multiplying by 50. For example, the average thickness swelling in the sampling zone located at 500mm away from both the left and top borders ($10^{th}$ row and $10^{th}$ column) is 25.3%, assuming additional 12% moisture absorption happened during exposure.

## 6.6. Degree of Orientation of Commercial OSB

As discussed before, the predicted degree of orientation of commercial OSB is 42.3%, assuming uniform flake size of 100 mm $\times$ 15 mm $\times$ 0.7 mm. The assumed flake geometry was made based on the visual observation on a commercial OSB panel because we cannot simply break the OSB into individual flakes and measure their geometry. **Figures** 6.9 and 6.10 indicate that the degrees of orientation decrease as the flake length and/or width increase if a constant characteristic area is maintained according to the degree of orientation equation (**Equation** 30) derived in **Chapter** III. Thus if either length and/or width deviate from the initial assumption, the corrected predicted value can be obtained from these **Figures**.

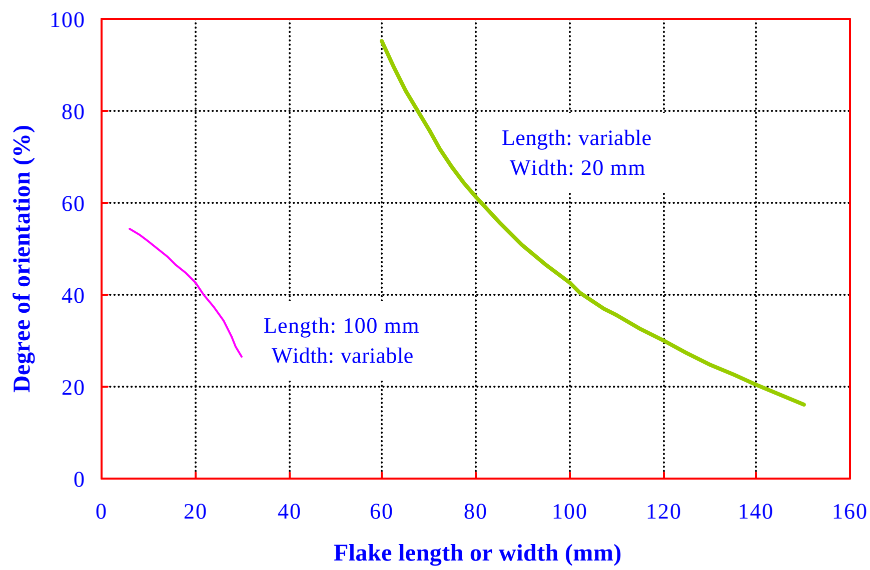


**Figure** 6.9 Degree of orientation of commercial OSB in corresponding to a constant characteristic area.

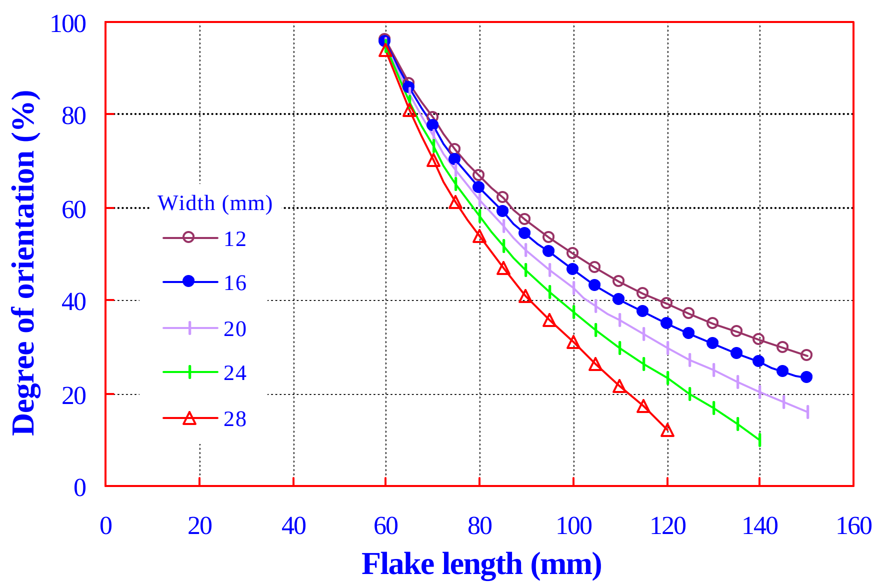


**Figure** 6.10 Degree of orientation of commercial OSB in corresponding to a constant characteristic area.

## 6.7. Future Research Work

The future work on expanding the present model could be as follows:

- Large OSB panels could be made by using a larger robot mat-forming system and an effective testing method to extract density information both horizontally and vertically can be developed.

- Strength property models, such as tension strength and modulus of elasticity could be developed, by incorporating the autocorrelation function and variance function into the models. Since the degree of orientation of the flakes can be determined from the autocorrelation function and the longitudinal strength of the panel is related to the orientation of flakes in the mat, a relationship between the MOE and autocorrelation may exist.

- The current simulation program could be expanded to incorporate the above strength prediction models. The next generation of the simulation will probably perform the opposite function, *i.e.*, input density and strength requirements to intelligently compute what kind of raw materials and structure are needed to achieve our target properties.

- The flake shift or movement could be considered during the mat forming and compressing processes because this will most likely happen in the real situation.

- The current model provides a methodology to be used to predict the thickness swelling in high relative humidity conditions. Further work needs to be done to expand this model to allow the prediction of thickness swelling for the commercial OSB panels

## 6.8. Limitations

There are a couple of limitations that need to be considered in the future studies:

- Wax and other additives could be added to the experimental mats to make them close to the commercial panels to reduce the moisture and/or water absorption during thickness swelling tests.
- Although the simulation program (***Winmat***©) allows the input of mixed flake sizes, the mathematical model can only take uniform flake geometry. Furthermore, the irregular shape of flakes could be considered in both simulation program and mathematical models.

## 6.9. References

Dai, C. and P. R. Steiner. 1994. Spatial structure of wood composites in relation to processing and performance characteristics. Part 3. Modeling the formation of multi-layered random flake mats. Wood Science and Technology. 28:229-239